1-21-2011

Inhibition of Proprotein Convertase Ski-1 Blocks Transcription of Key Extracellular Matrix Genes Regulating Osteoblastic Mineralization

Jeff P. Gorski
University of Missouri

Nichole T. Huffman
University of Missouri

Sridar Chittur
University at Albany

Ronald J. Midura
Lerner Institute

Claudine Black
University of Missouri

See next page for additional authors

INHIBITION OF PROPROTEIN CONVERTASE SKI-1 BLOCKS TRANSCRIPTION OF KEY EXTRACELLULAR MATRIX GENES REGULATING OSTEOBLASTIC MINERALIZATION

Jeff P. Gorski[1], Nichole T. Huffman[1], Sridar Chittur[2], Ronald J. Midura[3], Claudine Black[1], Julie Oxford[4], and Nabil G. Seidah[5]

From the [1]Center of Excellence in the Study of Musculoskeletal and Dental Tissues and Dept. of Oral Biology, Sch. Of Dentistry, Univ. of Missouri-Kansas City, 650 East 25th Street, Kansas City, MO 64108, [2]Center for Functional Genomics, Univ. at Albany, Rensselaer, NY 12144, [3]Dept. of Biomedical Engineering, Lerner Institute, Cleveland Clinic, Cleveland, OH 44195, [4]Dept. of Biology, Boise State Univ., Boise, ID 83725, and [5] Biochemical Neuroendocrinology, IRCM, Montréal, Québec, H2W 1R, Canada

Address correspondence to: Jeff P. Gorski, Ph.D., Bone Biology Program, Center of Excellence in the Study of Musculoskeletal and Dental Tissues, Dept. of Oral Biology, Sch. Of Dentistry, Univ. of Missouri-Kansas City, 650 East 25th Street, Kansas City, MO 64108. Phone: 816-235-2537; Fax: 816-235-5524; Email: gorskij@umkc.edu

Mineralization, a characteristic phenotypic property of osteoblastic lineage cells, was blocked by AEBSF and dec-RRLL-cmk, inhibitors of SKI-1 (site 1; subtilisin kexin like-1) protease. Since SKI-1 is required for activation of SREBP and CREB/ATF family transcription factors, we tested the effect of these inhibitors on gene expression. AEBSF decreased expression of 140 genes by 1.5- to 3.0-fold including *Phex, Dmp1, COL1A1, COL11A1* and *fibronectin*. Direct comparison of AEBSF and dec-RRLL-cmk, a more specific SKI-1 inhibitor, demonstrated that expression of *Phex, Dmp1, COL11A1* and *fibronectin* was reduced by both while *COL1A2* and *HMGCS1* were reduced only by AEBSF. AEBSF and dec-RRLL-cmk decreased the nuclear content of SKI-1 activated forms of transcription factors SREBP-1, SREBP-2, and OASIS. In contrast to AEBSF, the actions of dec-RRLL-cmk represent the sum of its direct actions on SKI-1 and indirect actions on caspase-3. Specifically, dec-RRLL-cmk reduced intracellular caspase-3 activity by blocking the formation of activated 19 kDa caspase-3. Conversely, over-expression of SKI-1 activated SREBP-1a and CREB-H in UMR106-01 osteoblastic cells increased the number of mineralized foci and altered their morphology to yield mineralization nodules, respectively. In summary, SKI-1 regulates the activation of transmembrane transcription factor precursors required for expression of key genes required for mineralization of osteoblastic cultures in vitro and bone formation in vivo. Our results indicate that the differentiated phenotype of osteoblastic cells, and possibly osteocytes, depends upon the non-apoptotic actions of SKI-1.

Bone formation and mineralization is a multi-step process of differentiated osteoblastic cells. Based upon an analysis of gene expression during osteogenesis, Lian and Stein (1) noted that "peak levels of expressed genes reflect a developmental sequence of bone cell differentiation characterized by three principal periods: proliferation, extracellular matrix maturation and mineralization, and two restriction points to which the cells can progress but cannot pass without further signals." These authors defined these three periods of osteoblastic differentiation in terms of patterns of sequential gene expression. For example, fibronectin and type I collagen expression denoted the pattern of pre-osteoblastic cells, alkaline phosphatase and MGP[6] reflected the matrix maturation stage, and, osteopontin and osteocalcin reflected the mineralization stage of mature osteoblastic cells (1). However, the number of genes required for normal bone formation and mineralization has grown rapidly to include Phex (*Phex*), dentin matrix protein1 (*Dmp1*), and type XI collagen (*COL11*).

Phex (phosphate regulating endopeptidase homolog, X-linked) is a transmembrane metalloendoprotease enriched on bone osteoblasts and osteocytes (2). It is essential for phosphate homeostasis and bone mineralization since loss of function mutations result in X-linked hypophosphatemic rickets (3). Acidic

phosphorylated dentin matrix protein 1 is highly expressed in teeth and osteocytes in bone. Mutations in *Dmp1* cause autosomal recessive hypophosphatemic rickets (4, 5). Elevated circulating levels of fibroblast growth factor 23 are a characteristic shared by both this human condition and by mice lacking Dmp1 (5). The hypophosphatemic rickets and elevated FGF23 levels that occur in *Dmp1* null mice resemble the 'hyp' mouse, which has an inactivating mutation in *Phex*. Since skeletal abnormalities in both these animal models can be largely but not completely rescued by feeding a high phosphate diet, DMP1 and Phex regulate an essential pathway controlling serum phosphate levels needed for mineralization of teeth and bone. Type XI collagen regulates the rate of fibrillogenesis of type I and II collagen and the ultimate size of fibrils (6). Homozygous *cho* mice containing a frame shift mutation in the COL11A1 gene die at birth with severe abnormalities of bone and tracheal cartilage (7). In humans, COL11A1 mutations cause Marshall and Stickler syndromes (8) characterized by craniofacial abnormalities, nearsightedness and hearing deficiencies. Finally, fibronectin is a multi-functional matrix organizing protein possessing binding sites for collagen, glycosaminoglycan chains, and cell adhesion receptors. Blocking antibodies against the fibronectin receptor inhibit the mineralization of osteoblastic cells in culture (9-11). Although genetic knockouts and mutations causing skeletal abnormalities have identified these and other genes, detailed mechanisms controlling bone formation and mineralization are incompletely understood.

We have used osteoblastic culture models to investigate the mechanism controlling bone mineralization (12-18). Mineralization occurs within spherical, macromolecular, extracellular, vesicle-enriched complexes termed biomineralization foci. Since BMF phosphoprotein biomarkers can be used to define areas of growing periosteum and developing fracture callus prior to their mineralization (14, 15), osteoblastic cultures appear to model bone formation in vivo. Proteomic analyses on laser micro dissected mineralized BMF show they are enriched in phosphoproteins BSP and BAG-75 and their fragments. Interestingly, both phosphoprotein cleavage and mineralization of BMF can be completely blocked with covalent serine protease inhibitor AEBSF, whereas 15 other inhibitors against acidic, metallo-, and sulfhydryl proteases were without effect (16). Based on these results, we hypothesized that initiation of bone mineralization is controlled by a serine protease. We recently showed that BMF contained an active, 105 kDa form of SKI-1 protease (18).

SKI-1 is a member of the proprotein convertase family (19). PCs, serine proteases related to bacterial subtilisin and yeast kexin, cleave and activate growth factors, neuropeptides, toxins, glycoproteins, viral capsid proteins, and transcription factors. Transmembrane transcription factor precursors SREBP-1 and -2 are activated in a sequential process involving first SKI-1 cleavage and then S2P protease cleavage (20). SREBPs can also be activated by caspase-3 (21, 22). The N-terminal fragments of SREBP-1 and SREBP-2 can then be imported into the nucleus where each regulates gene expression by binding to promoters containing consensus SRE sequences (23). Members of the CREB/ATF family of transcription factors [ATF-6, LUMAN (CREB3), OASIS/BBF2H7 (CREB3L2), CREB-H, CREB-4, and AIbZIP/Tisp40 (CREB3L4)] also require SKI-1 catalyzed activation. By activating ATF-6, SKI-1 serves as an initiator of the unfolded protein response which decreases cellular stress by increasing chaperone production, influencing ER-associated degradation of proteins, and regulating membrane remodeling (24).

Recent studies indicate that SKI-1 is required for normal bone formation. First, the skeletons of mice deficient in OASIS (25) exhibit a severe osteopenia characterized by a type I collagen-deficient bone matrix and reduced osteoblastic activity (26). Second, mice over-expressing ICER, a dominant negative effector of CREB/ATF transcription factors, displayed dramatically reduced trabecular bone and a reduced femoral bone formation rate (27). Third, SKI-1 is required for normal cartilage morphogenesis in zebrafish (28). Finally, conditional inactivation of SKI-1 in mice using a type II collagen Cre recombinase transgene leads to abnormal growth plate calcification (29).

The purpose of this study was to determine whether SKI-1 protease controls initiation of osteoblastic mineralization.

EXPERIMENTAL PROCEDURES

Growth, mineralization and treatment of UMR cells with protease inhibitors. UMR 106-01 BSP cells were passaged and cultured as described

previously (12). Cells were seeded at a density of 1.0 x 10^5 cells/cm^2 in Growth Medium. After 24 h, Growth Medium containing 0.5% BSA (Millipore #82-045-1) was exchanged for FBS containing medium. Sixty-four hours after plating, spent medium was exchanged with Mineralization Media (Growth Medium containing 0.1% BSA and 6.5 mM BGP). Addition of a supplemental phosphate source to UMR 106-01 cultures prior to 64 h had no effect on the formation of mineral crystals (Midura and Gorski, manuscript in preparation). Cultures were then incubated for up to an additional 24 h at which time they were fixed with 70% ethanol.

In some experiments, serine protease inhibitor AEBSF (EMD Biosciences, Inc.) or dec-RRLL-cmk (Bachem, Inc.) was added over a range of concentrations in Mineralization Media at 64 h after plating. We have shown previously (16) that 100 µM AEBSF is the minimum dosage able to effectively block mineralization of BMF within serum-depleted UMR cultures.

The extent of mineralization was either assessed visually by fluorescence microscopy (after staining with 10 µg/ml Alizarin red S dye) or quantitated by colorimetric calcium assay (17) by reference to a standard curve. In the latter case, calcium was first extracted from culture wells with acidified 70% ethanol and the extracts were then concentrated prior to analysis.

Transgenic DMP1 GFP mice were kindly provided by Drs. I. Kalajzic and D.W. Rowe, University of Connecticut Health Center.

SDS gel electrophoresis and Western blotting. Protein samples were electrophoresed under reducing conditions on 4-20% linear gradient gels (Pierce Chem. /Thermo Scientific) according to Laemmli (30) and electro blotted onto PVDF membranes (Millipore Corp.) for 1.5-2 h at 100 volts in 10 mM CAPS buffer (pH 11.0) containing 10% methanol. Blots were processed with primary antibody and horseradish peroxidase-conjugated secondary antibody as described previously (17) and chemiluminescent digital images captured with a Fuji LAS-4000.

Anti-SKI-1 antibodies [h-SKI-CT (C-terminal specific for aa 1036-1051); 723.03 (recognizes pro-SKI-1); 705.02 (recognizes residues 634-651)] [see Pullikotil et al. (31, 32) for details] and anti-CREB-H antibodies (33) were a gift from Dr. K Zhang, Wayne State Univ. Antibodies against SREBP-1 (aa 38-89), SREBP-2 (aa 424-473), and GAPDH were purchased from Sigma Chemical Inc. while antibodies against OASIS were obtained from Aviva Systems Biology.

Isolation of nuclear and cytoplasmic fractions from UMR 106-01 cultures. UMR 106-01 cells were cultured under serum depleted conditions as described above. Sixty-four hours after plating, the medium was exchanged for Mineralization Medium (18); some of the cultures were also treated with 100 µM AEBSF, 40 µM dec-RRLL-cmk, 10 µM Z-DEVD-fmk or 20 µM Z-DEVD-fmk. Cultures were then incubated for an additional 12 hours and then the nuclear and cytoplasmic fractions were prepared using a Thermo Scientific NE-PER Nuclear and Cytoplasmic Extraction kit per the manufacturer's instructions. Extracts were aliquoted and stored at -80°C until subjected to Western blotting.

Transfection with plasmids. UMR 106-01 cells were plated in 24 well plates with Growth Medium containing 10% FBS. At 40 h after plating, transfections were carried out in Growth Medium containing 1% FBS. Initially, each plasmid was pre-titered to determine an optimum dosage; cell cultures were transfected with 0.25-0.75 µg of plasmid DNA at three different levels of Metafectene Pro transfection reagent (Biontex) per manufacturer's protocol. Individual plasmids and Metafectene Pro reagent were pre-incubated at room temperature for 20 minutes prior to addition to cells for 24 hrs at which time the mixture was exchanged for serum-free Mineralization Medium containing 0.1% BSA. An optimized dosage of plasmid was used in subsequent studies examining the effect of over-expression of recombinant transcription factors on mineralization. At 88 hrs after plating, cultures were fixed in 70% ethanol and then stained with 10 µg/ml Alizarin red S dye. Both bright field and fluorescence microscopic images were obtained. Alternatively, calcium was quantitated with a colorimetric assay (16).

Expression plasmids were prepared as follows. cDNAs coding for hSREBP-1a, -1c and -2 were purchased from Origene. PCR was used to clone their N-terminal fragments and to then tag them with the V5 epitope (GKPIPNPLLGLDST) at their C-terminus. The resultant plasmids produced the following proteins: hSREBP1a = aa 1-511-V5; SREBP-1c = aa 55-511-V5; and, SREBP-2 = aa 1-475-V5. [Expression plasmids OASIS TMC-HA tag, OASIS TMC, and CREB-H TMC were kindly provided by Dr. P. O`Hare (Marie Curie Research Institute, United Kingdom)].

Extraction of proteins from UMR 106-01 cultures. UMR 106-01 cells were seeded in 48-well plates and grown in serum depleted conditions as described previously (16, 17). During the final 24 h mineralization period, wells were exchanged with Mineralization Medium containing 0.1% BSA; some of the wells also received 100 μM AEBSF or 40 μM dec-RRLL-cmk. At the conclusion of the culture period, media was removed, inactivated at 95°C for 5 min, dialyzed against 5% acetic acid, and lyophilized to dryness. The cell layer was extracted as previously described (16); EDTA extracts were immediately inactivated at 95 and processed as described above. Subsequent Urea/CHAPS cell layer extracts (16) were homogenized and then ultracentrifuged at 30,000 rpm (~100,000 x g) for 1 h in an SW50.1 rotor prior to SDS PAGE and Western blotting studies.

Laser micro dissection of BMF. UMR 106-01 cells were plated onto glass slides, mineralized, and processed for laser micro dissection, extraction and Western blotting as described by Huffman et al. (16).

Primary calvarial cell isolation and cell culture. Primary mouse osteoblasts were isolated from calvaria of 5- to 7-day-old transgenic DMP1 GFP mice (34) using a modification of a published method (35, 36). Briefly, four sequential 20-min digests were performed in Hanks' balanced salt solution containing 0.05% trypsin and 0.2% collagenase. Fractions 2 to 4 were pooled, centrifuged, and re-suspended in α-MEM medium containing 10% FBS, 2 mM L-glutamine, 100 units/ml penicillin, and 30 μg/ml gentamicin (α-Growth Medium). 2×10^6 cells were plated per T-75-cm^2 flask and allowed to reach confluency. Flasks were then trypsinized and the cells plated onto 48-well culture dishes. At confluency, the media was changed to α-MEM containing 5% FBS, 50 μg/ml ascorbic acid, 5 mM beta-glycerolphosphate, and antibiotics. BGP was omitted from wells that served as un-mineralized controls.

Some cultures were treated on days 6 and 9 with 8 μM dec-RRLL-cmk or 10 μM AEBSF. On day 12, cultures were either incubated with MTT or were fixed with 2% p-formaldehyde and processed for Alizarin red S staining. Images were taken with a Nikon T2000 fluorescence microscope equipped with a CCD camera.

DNA array. Triplicate UMR 106-01 cultures were plated (13, 16) and grown with or without 400 μM AEBSF for 12 h prior to isolation of total RNA (~5 μg) and then converted to single stranded cDNA using Superscript II reverse transcriptase (InVitrogen, Inc.) and the Gene Chip T7 promoter primer kit. [Note: the minimum effective dose of AEBSF capable of completely blocking mineralization in UMR 106-01 cultures is 100 μM in serum free media and 400 μM in media containing 10% FBS (16)]. Single stranded cDNA was then converted to double stranded cDNA using DNA polymerase I DNA ligase and RNase H from *E. coli*. The double stranded cDNA was purified using a cleanup kit from Affymetrix and converted to biotinylated cRNA by *in vitro* transcription using T7 polymerase and biotinylated ribonucleotides (Affymetrix). This was subsequently fragmented by metal induced hydrolysis to yield 35-200 base fragments that were hybridized to the Affymetrix Rat Genome 230 Plus 2.0 oligonucleotide arrays. After hybridization, the chip was washed and stained with streptavidin-phycoerythrin before being scanned. An antibody amplification staining protocol that used biotinylated goat IgG followed by a second SAPE staining increased the sensitivity of the assay. The chip was then scanned and images analyzed qualitatively using Affymetrix Gene Chip Operating System Software.

Microarray data analysis. CEL data files were imported into Gene Spring GX software (v10) and the data was normalized using either the MAS5 or the GCRMA algorithm. The gene list was filtered to exclude those which showed low signal values across all samples (i.e. bottom 20th percentile). Selection of statistically significant genes from each expression profile was done using an unpaired t-test with a p-value cut off of < 0.05. The multiple testing correction (Benjamini and Hochberg false discovery rate, p-value <0.05) was integrated within each test. Differential expression was defined as $\geq$1.5-fold change in expression found using both MAS5 and GCRMA analysis. Using this stringent criteria avoids false positives associated with use of MAS5 alone as well as well as facilitates the ability of GCRMA to account for non-specific hybridization related background signal.

Isolation of RNA from serum depleted osteoblastic cultures and conversion to cDNA. UMR 106-01 cells were plated and grown under serum depleted conditions (13, 16). At 64 h after plating, the media was exchanged with serum-free

Mineralization Media. At 76 h after plating, media was removed from each well and cells were quickly lysed with STAT-60 (Tel-Test, Inc.); the lysates were then immediately frozen and stored in liquid nitrogen vapor. Total RNA was isolated according to manufacturer's instructions (Tel-Test, Inc.). Each RNA pellet was washed 2 times with 80% ethanol and then air dried prior to re-suspending in 10 µl RNase-free water containing 4% RNAsin inhibitor (Promega, Inc.). cDNA was produced using the High Capacity cDNA Reverse Transcription Kit (Applied Biosystems) and stored frozen in aliquots.

For real time PCR, cDNA preparations were diluted and added to 96-well plates containing Taqman Master Mix solution and either the appropriate FAM-(6-carboxyfluorescein)-labeled expression gene primer set or the VIC-labeled β-actin control primer set (ABI, Inc.). Plates were run on an ABI 7000 Real Time system using pre-programmed software. All calculations were made by the Delta-Delta CT method by comparison to the β-actin control.

Assay of Caspase-3. Recombinant caspase-3 (Sigma Chem. Co.) and lysates of UMR106-01 cultures were assayed using a fluorescent substrate and reagents from Ana-Spec, Inc. (#71118) according to the manufacturer's protocol.

Assay of SKI-1 Peptidase Activity. UMR106-01 cultures were cultured as usual in 48-well plates and treated with inhibitors as described above. The media was exchanged for serum-free medium and then the total cell layer was disrupted by scraping into reaction buffer and aliquots were immediately assayed using a succinylated TISRRLL-MCA substrate (37) and a fluorescent plate reader at 0, 0.5, 1, and 2 h. Rates were extrapolated from kinetic reaction curves.

RESULTS

Activated 105 kDa form of SKI-1 is present in biomineralization foci. SKI-1 protease is synthesized as a membrane bound precursor of 145 kDa (38) and is activated by autolytic cleavage to generate catalytically active 105 kDa (membrane bound) and 98 kDa (shed) forms (38, 39). SKI-1 can be inactivated by the irreversible covalent serine protease inhibitor AEBSF. Since we showed previously that AEBSF blocked mineralization and inhibited fragmentation of BMF biomarkers BSP and BAG-75 (16), we asked if active SKI-1 is associated with extracellular biomineralization foci and whether AEBSF alters the distribution of SKI-1 within mineralizing cultures.

Mineralized BMF were isolated by laser micro dissection from UMR 106-01 cultures and Western blotted with a polyclonal antibody recognizing the C-terminal cytosolic tail of SKI-1 (32). Only the 105 kDa form was present in BMF isolated from mineralized cultures (lane BMF, Fig. 1A). In contrast, the CL-Min and CL-UnMin lanes contained the 105 kDa band along with presumed fragments at 70 and 50 kDa (Fig. 1A). However, the 70 and 50 kDa components were not detected in micro dissected BMF. While the BMF fraction contains only mineralized foci (Fig. 1) (16), CL-Min and CL-UnMin fractions represent extracts of the cell layer from mineralized and un-mineralized cultures, respectively, which includes cells and BMF.

Cell layers were extracted with a two step protocol devised to efficiently extract proteins from cells and the extracellular matrix. Mild EDTA extraction predominantly removes materials associated with extracellular BMF complexes, whereas extraction with 8M urea/CHAPS recovers residual intracellular and extracellular matrix components (16). Activated 105 kDa SKI-1 was present in the EDTA extract but absent from AEBSF-treated or un-mineralized cultures (Fig. 1B) suggesting transport of SKI-1 to extracellular BMF occurs only during mineralization. Urea/CHAPS extracts contained similar amounts of 105 kDa SKI-1 regardless of the culture condition. The culture media contained 145 kDa SKI-1 precursor and a 50 kDa fragment band. Due to the specificity of the antibody and the structure of SKI-1 (31, 32, 38, 39), we assume that all forms detected (145, 105, 70, and 50 kDa) contain the transmembrane sequence and are associated with membranes or vesicles released from cells. Interestingly, the amount of 50 kDa band in the media was found to be lower in mineralized cultures indicating that breakdown of SKI-1 may be increased under non-mineralizing conditions (Fig. 1B).

Treatment of osteoblastic cultures with a specific SKI-1 inhibitor also blocks mineralization. The structure of dec-RRLL-cmk is based on the preferred substrate specificity of SKI-1 and is more specific than AEBSF (32, 37, 38). When UMR106-01 cells were treated with dec-RRLL-cmk, mineralization was progressively blocked as the concentration of inhibitor was increased (Fig. 2A). Forty micromolar dec-RRLL-cmk represents

a minimum effective inhibitory dose compared with 100 μM AEBSF (Fig. 2A and B) (16). By contrast, a structurally similar furin inhibitor (40), dec-RVKR-cmk, was without effect (Fig. 2C). Importantly, assays of treated cultures also demonstrated that AEBSF and dec-RRLL-cmk significantly decreased SKI-1 peptidase activity by about 30 and 40%, respectively, while treatment with other inhibitors containing analogous reactive functional groups were without a negative effect (Table 1). AEBSF and dec-RRLL-cmk do not significantly decrease cell number (Fig 1) (16), while Z-DEVD-OPH and dec-RVKR-cmk reduce cell viability by no more than 15% (not shown).

We also treated primary calvarial osteoblastic cultures from transgenic DMP1-GFP mice (34-36) with dec-RRLL-cmk. Since GFP expression precedes mineralization in these cultures, this protein serves as a marker of where and when mineralization will occur in these longer term cultures. Osteoblastic precursors were plated onto collagen coated wells and grown under mineralizing conditions for up to 12 days in the presence of either 0, 1, or 8 μM dec-RRLL-cmk. Concentrations of AEBSF and dec-RRLL-cmk were lowered to accommodate the longer exposure with primary cells versus UMR 106-01 cells. Mineral crystals were detected by staining with Alizarin red S and correlated with GFP expression. Focal areas of GFP-positive cells generally appeared about 6-8 days after plating and go on to form mineralized nodules by about day 12 (Fig. 3A). Exposure to 8 μM dec-RRLL-cmk inhibitor diminished expression of the DMP1-GFP reporter (Fig. 3B), as well as blocking mineralization. As a positive control, 10 μM AEBSF also completely blocked mineralization and DMP1-GFP reporter expression by primary calvarial cultures (16) (Fig. 3C). These results indicate that SKI-1 is required for progression through the osteoblastic mineralization stage and the transition to the embedded osteoblast or osteocyte stage.

Short-term treatment of osteoblastic cells with AEBSF decreases transcription of mineralization-related genes. Since SKI-1 and S2P catalyze the release of activated transcription factors from the cis/medial Golgi (19), we asked whether AEBSF blocks transcription of mineralization related genes. UMR106-01 cultures were treated for 12 h (from 64-76 h after plating) with or without a minimum concentration of AEBSF sufficient to block mineralization. UMR106-01 cultures begin to nucleate calcium phosphate crystals within biomineralization foci at 76 h (16, 17). Total RNA was isolated, converted to cDNA prior to labeling and incubated with whole rat genome arrays (see EXPERIMENTAL PROCEDURES for details).

AEBSF treatment reduced expression of 140 genes by 1.5 to 3-fold while twenty-eight genes were found to be increased by at least 1.5-fold [Array data has been deposited with the Gene Expression Omnibus database (series accession number GSE21476)]. It is noteworthy that genes encoding a number of mineralization related extracellular matrix proteins were reduced (Table 2), e.g., DMP1, type I procollagen alpha 1 and alpha 2 chains, type XI procollagen alpha 1 chain, fibronectin, matrilin 3, ectonucleotide pyrophosphatase/phosphodiesterase 2 and 3, and tenascin-C and -N. Interestingly, the reduced expression for *DMP1* observed (Table 2) is consistent with the lack of DMP1-GFP transgene expression noted in primary calvarial cultures treated with these inhibitors (Fig. 3).

Dec-RRLL-cmk also blocks transcription of Dmp1, Phex, FN1, COL11A1 genes. Because dec-RRLL-cmk is a more specific inhibitor of SKI-1 than AEBSF (20), we predicted that it should reproduce those actions of AEBSF (Table 2) which are mediated by SKI-1. To test this, UMR106-01 cultures were again treated for 12 h with 40 μM dec-RRLL-cmk (Fig. 2). Parallel cultures were also treated with AEBSF (16) (Fig. 2B). This study was carried out under conditions of serum deprivation to reduce exposure to cholesterol which inhibits SCAP-mediated transport of SREBPs towards the cis/medial Golgi where they are activated by SKI-1 and S2P (41). We showed earlier that the amount of mineral deposited in UMR106-01 cultures is unaffected by serum depletion (16).

Total RNA was isolated and converted to cDNA. Quantitative PCR was then carried out on a representative group of genes decreased by AEBSF (Table 2). Expression of HMG-CoA synthase (HMGCS1) was also included as a positive control since it is regulated by SREBP transcription factors activated by SKI-1 (42, 43). Other cultures were treated with inhibitors until 88 h when the amount of mineralization was determined. As expected, both inhibitors blocked mineralization by greater than 90% (data not shown but similar to that in Figure 2B).

All qPCR results are plotted in Figure 4 as a percentage of the expression in cultures treated

with mineralizing conditions. Visual inspection of the data reveals two patterns. First, expression of *DMP1, procollagen XI alpha 1 chain, Phex,* and *fibronectin* was significantly decreased by each SKI-1 inhibitor (Figs. 4A-D). For each gene, the average knockdown with AEBSF was found to be quantitatively greater than that for dec-RRLL-cmk (Figs. 4A-D), but differences were not significant. In the second pattern, highest expression of *COL1 A2* and *HMGCS1* occurred in dec-RRLL-cmk treated cultures whereas that for mineralizing control or for AEBSF-treated culture was found to be significantly lower (Fig. 4E and F). Expression of *HMGCS1* in AEBSF treated cells was indistinguishable from controls (+BGP, Fig. 4E), whereas expression of *COL1 A2* was lower in AEBSF treated cells than controls (+BGP vs. AEBSF, p=0.05, Fig. 4E). The qPCR results with AEBSF are very similar to array results for *DMP1, procollagen XI alpha 1 chain, Phex, fibronectin,* and *COL1 A2* (Table 2). The results for *HMGCS1* were unexpected since its expression is tightly regulated by SREBP-1 and SREBP-2 (42, 43) and thus should be dependent upon SKI-1. Based on qPCR results, mineralization in UMR106-01 cultures correlates most closely with the expression of *DMP1, COL11 A1, fibronectin*, and *Phex* (compare Figs. 2 and 4).

Activation of caspase-3 is regulated differently in AEBSF and dec-RRLL-cmk treated cultures. As first shown by Wang et al. (20, 21), activation of SREBP-1 and SREBP-2 can be also mediated by caspase-3. Caspase-3 and SKI-1 cleave these factors at different sites producing different sized, transcriptionally active N-terminal fragments (21, 22). We therefore tested whether a caspase-3/-7 specific inhibitor would also inhibit mineralization of BMF. Interestingly, 10 and 20 μM Z-DEVD-fmk had no significant effect on mineralization in UMR06-01 cultures (Fig. 5A). By comparison, 100 μM AEBSF and 50 μM dec-RRLL-cmk blocked mineralization by >85% (Fig. 5A).

To determine if caspase-3 was specifically inactivated by Z-DEVD-fmk, the cytosolic fraction of cell lysates was assayed using a small fluorescent peptide substrate. Caspase-7 is predominantly membrane bound (44) under these conditions and should have been removed by centrifugation prior to assays. Intracellular caspase-3 catalytic activity was blocked by up to 80% by Z-DEVD-fmk and was also reduced about 60% by dec-RRLL-cmk (Fig. 5B). However, AEBSF had no effect. To establish if dec-RRLL-cmk directly inactivated caspase-3, we incubated recombinant caspase-3 with various inhibitors for 30 min and then measured its catalytic function. As shown in Figure 5C, 50 μM dec-RRLL-cmk and 100 μM AEBSF were all without effect—suggesting that the former acts indirectly to block procaspase-3 activation.

In view of the differential gene expression patterns observed with AEBSF and dec-RRLL-cmk treated osteoblastic cultures (Fig. 4), we next asked whether the amount of activated caspase-3 protein varied as a function of the inhibitor used. UMR106-01 cultures were treated for 12 h with a series of inhibitors as described in Figure 4. Cell layers were then dissociated in hot SDS-8M urea solution containing an excess of DTT, and fractions were processed for Western blotting. The total cellular content of activated 19 kDa caspase-3 (45) was similar in mineralizing, un-mineralized, and AEBSF–treated cultures (Fig. 5D). However, the caspase-3 content of dec-RRLL-cmk treated cultures was greatly reduced (arrow, Fig. 5D). By comparison, blots processed for control protein GAPDH gave similar band intensities for all conditions (Fig. 5E). These results also suggest that activation of procaspase-3 is decreased in dec-RRLL-cmk treated cultures compared with mineralizing, un-mineralized, and AEBSF–treated cultures. Finally, the content of 19 kDa caspase-3 was noticeably higher in cultures treated with 10 and 20 μM Z-DEVD-fmk or Z-DEVD-OPH than in controls (arrowheads, Fig. 5D).

Treatment of UMR106-01 cells with AEBSF or with dec-RRLL-cmk alters the nuclear content of SKI-1 activated transcription factors. To further test if SKI-1 is required for activation of SREBP and CREB/ATF family transcription factors which are imported into the nucleus where they control the expression of mineralization related genes, we asked whether AEBSF or dec-RRLL-cmk reduced the nuclear content of selected transcription factors. Commonly, cells grown in 10% fetal bovine serum have been used as a control for caspase-3 activation since the serum cholesterol leads to feedback inhibition of SKI-1 activation of SREBPs. As a result, Western blotting was used to identity the activating protease from the nuclear sizes of activated transcription factors

To select which transcription factors to investigate, we searched for conserved transcription factor binding sites in the proximal promoter regions of the *PHEX, DMP1, FN1,*

COL11A1, COL1A2, and *HMGCS1* genes using the NCBI ECR Browser program. This analysis revealed that consensus SRE and CRE sequences exist in all of the six 5'-proximal promoter regions (not shown). Additionally, OASIS was shown recently to be required for normal bone formation (25, 26) and CREB-H (CREB3L3) represents a CREB/ATF family member activated by SKI-1 (33). Expression of HMGCS1 is also regulated primarily by SREBP-1 and SREBP-2 (42, 43). Based on these findings, we focused our analyses on a mix of SRE and CRE binding factors: SREBP-1, CREB-H (CREB3L3), OASIS (CREB3L1), and SREBP-2.

UMR106-01 cells were plated as usual in 10% fetal bovine serum (16) and at 64 h the media was exchanged again for serum free media containing either BGP alone (mineralizing conditions) or with AEBSF, dec-RRLL-cmk, or Z-DEVD-fmk. Since AEBSF and dec-RRLL-cmk required only 12 h to reduce transcription of key mineralization genes (see Fig. 4), we also stopped these cultures 12 h after addition of inhibitors. Nuclear (Fig. 6) and cytoplasmic (Fig. 7) fractions were then immediately prepared for Western blotting.

Nuclear OASIS consisted of a 58 kDa SKI-1 activated form (OASIS panel, Fig. 6). This assignment is consistent with the findings of Omori et al. (46). The nuclear content of 58 kDa OASIS was lower in both the AEBSF and dec-RRLL-cmk treated cultures (OASIS panel, Fig. 6). Parallel controls with cytoplasmic extracts from these same cultures were blotted against GADPH and show that the observed changes were not due to differences in sample loading (see Fig. 7). These results indicate that AEBSF and dec-RRLL-cmk both reduce the nuclear content of SKI-1 activated 58 kDa OASIS.

In contrast to OASIS, the nuclear content of CREB-H did not change when AEBSF or dec-RRLL-cmk was included. Consistent with other work with this antibody (32), a 42 kDa band (SKI-1 activated) and doublet immunoreactive bands containing 42 (SKI-1 activated) and 45 kDa (caspase-3 activated) forms were detected in +FBS cultures (CREB-H panel, Fig. 6). Thus, CREB-H does not play a role in transcriptional changes brought about by AEBSF or dec-RRLL-cmk (Fig. 4).

The nuclear content of 68 kDa activated SREPB-2 was reproducibly decreased by both AEBSF and dec-RRLL-cmk (SREBP-2 panel, Fig. 6). By comparison, nuclei from +FBS treated cultures contained two closely spaced activated SREPB-2 forms at 68 kDa (SKI-1 cleavage) and at 65 kDa (presumed to be cleaved by caspase-3). The nuclear content of 68 kDa SREBP-2 is reduced in cultures treated for 12 h with either AEBSF or dec-RRLL-cmk.

SKI-1 activated SREBP-1 is also 68 kDa (20, 21) as shown in the mineralized control (SREBP-1 panel, Fig. 6). This band is largely absent in non-mineralizing conditions (No Phosphate, AEBSF, and dec-RRLL-cmk) (SREBP-1 panel, Fig. 6). A separate 58 kDa form of SREBP-1 (produced by caspase-3) is present in +FBS cultures (20, 21).

In order to confirm the assignment of caspase-3 cleaved transcription factors in Figure 6, we isolated nuclear and cytoplasmic fractions from osteoblastic cultures treated with 10 and 20 μM Z-DEVD-fmk (Figs. 6 and 7). Our results show that the nuclear content of CREB-H was increased in cultures treated with 20 μM as compared with +BGP alone (CREB-H, panel, Fig. 6). The 42 kDa size of the activated nuclear CREB-H form whose content increased with 20 μM Z-DEVD-fmk is consistent with its cleavage by SKI-1 (CREB-H panel, Fig. 6).

The effect of AEBSF and dec-RRLL-cmk inhibitors on cytoplasmic SKI-1 activated transcription factors. Cytoplasmic transcription factor analysis provides a useful comparison with the nuclear profiles presented in Figure 6. While carried out in triplicate, single representative patterns are presented in Figure 7. In contrast to the nuclear results, the content of cytoplasmic 58 kDa OASIS did not appear to correlate with the presence or absence of inhibitors (Fig. 7). Cytoplasmic CREB-H consisted only of the SKI-1 activated 42 kDa form (33) and its content also did not vary in the presence of inhibitors (CREB-H panel, Fig. 7). In support of this assignment, the 42 kDa form was absent from +FBS cultures.

In contrast to results with nuclear fractions, analyses for cytoplasmic SREBP-2 revealed no detectable band under any culture condition (SREBP-2 panel, Fig. 7). Also, Western blotting results for SREBP-1 yielded faint doublet bands at 68 (SKI-1 activated) and 58 kDa (caspase-3 activated) primarily in the FBS and Z-DEVD-fmk treated cultures (SREBP-1 panel, Fig. 7). However, the content of cytoplasmic SREBP-1 forms did not change with inhibitors. Finally, the content of control protein GAPDH in cytoplasmic extracts was constant among the different conditions (GADPH panel, Fig. 7)

Over-expression of SKI-1 activated SREBP-1 increases mineralization in UMR106-01 cultures. To further test our hypothesis that osteoblastic mineralization is dependent upon SKI-1 catalyzed activation of SREBP and CREB/ATF family transcription factors, we transiently over-expressed SKI-1 activated transcription factors (SREBP-1a, SREBP-1c, SREBP-2, OASIS, and CREB-H) in UMR106-01 cells. Plasmids were used which express active transcription factors retaining their nuclear import sequences and bZIP DNA binding domains but missing their C-terminal membrane insertion sequences. All plasmids were compared over the same transfection dosage range which was optimized for SREBP-1a in initial titration studies. Results are presented visually in Figure 8 after fluorescent staining for calcium mineral with Alizarin red S.

Over-expression of SREBP-1a resulted in a significant increase in mineralized BMF complexes compared with the non-plasmid control or with cells transfected with OASIS, SREBP-2, or SREBP-1c (Fig. 8). In a separate experiment, SREBP-1a transfected cells contained 1.32-fold more calcium in mineral deposits compared with the non-plasmid control ($p<0.05$). Thus, over-expression of SREBP-1a was able to increase both the number of biomineralization foci and the amount of calcium mineral deposited by UMR 106-01 osteoblastic cells. Also, CREB-H transfected UMR 106-01 cells exhibited an unusual morphological appearance. In contrast to their usual dispersed appearance, BMFs in CREB-H transfected cells were clumped together in discrete regions which resembled mineralization nodules seen in primary calvarial osteoblastic cultures (see Fig. 3).

DISCUSSION

We show here that mineralization, a property of differentiated osteoblastic cells, is blocked by covalent serine protease inhibitors AEBSF and dec-RRLL-cmk in two osteoblastic culture models. Since both inhibitors inactivate SKI-1, an intracellular cis/medial-Golgi protease required for activation of SREBP and CREB/ATF family transcription factors, we examined the effect of these inhibitors on gene expression. Short term (12 h) treatment of osteoblastic cultures with AEBSF decreased expression of 140 genes by 1.5- to 3.0-fold including *Phex*, *Dmp1*, *COL1A1*, *COL1A2*, *COL11A1*, and *fibronectin*. A subsequent comparison of AEBSF with dec-RRLL-cmk, a more specific SKI-1 inhibitor, on expression of a subset of these genes revealed two different outcomes. *Phex*, *Dmp1*, *COL11A1*, and *fibronectin* were significantly reduced by both inhibitors. *COL1A2* and *HMGCS1*, a positive control for SKI-1 activity (42, 43), were also inhibited by AEBSF, but in contrast, expression was increased by dec-RRLL-cmk relative to mineralizing cultures. AEBSF and dec-RRLL-cmk also reduced the nuclear content of activated forms of OASIS, SREBP-1, and SREBP-2. Because caspase-3 is known to activate SREBP-1 and SREBP-2 (20, 21), we also tested caspase-3/capase-7 inhibitors; but Z-DEVD-fmk did not block osteoblastic mineralization. However, the activation and turnover of caspase-3 was differentially modified depending upon the inhibitor used, e.g., AEBSF, dec-RRLL-cmk, or Z-DEVD-fmk. In contrast to AEBSF, the actions of dec-RRLL-cmk represent the sum of its direct actions on SKI-1 and indirect actions on caspase-3. Specifically, dec-RRLL-cmk reduced intracellular caspase-3 activity by blocking the formation of activated 19 kDa caspase-3. Finally, over-expression of the SKI-1 activated forms of SREBP-1a and of CREB-H in UMR106-01 osteoblastic cells increased the number of mineralized foci and altered their local distribution, respectively. These findings suggest that expression of key genes (*Phex*, *Dmp1*, *COL11A1*, and *fibronectin*) needed for mineralization of osteoblastic cultures in vitro and for bone formation in vivo are regulated by SREBP and CREB/ATF family transcription factors which require SKI-1 for their activation.

Intracellular and extracellular roles for SKI-1 in osteoblastic mineralization. Mineralization in UMR106-01 cultures is a temporally synchronized process and the first mineral crystals begin to form 12 h after addition of exogenous phosphate (13, 16, 17). If phosphate is not added or if AEBSF is included, mineralization does not occur (16, 17). AEBSF also blocks the fragmentation of phosphoproteins BSP and BAG-75 which are enriched within biomineralization foci, along with inhibiting activation of procollagen C proteinase enhancer protein. These results suggest that 105 kDa SKI-1 may be responsible for extracellular proteolytic processing of secreted proteins within biomineralization foci.

Since intracellular SKI-1 can also activate transmembrane transcription factor precursors, we carried out a whole genome array comparison of

mineralizing versus AEBSF treated cultures. Transcription of one-hundred forty genes was reduced by 1.5- to 3-fold including *Phex*, *Dmp1*, *fibronectin*, *tenascin-N*, *tenascin-C*, *COL11A1*, *COL1A1*, and *COL1A2*. This result was then validated when six of these genes were retested with a more specific inhibitor of SKI-1, dec-RRLL-cmk, using a qPCR approach. Furthermore, treatment of primary cultures of transgenic DMP1-GFP calvarial cells with both SKI-1 inhibitors not only blocked mineralization but also inhibited GFP expression driven by a 10 kb DMP1 promoter. These findings demonstrate for the first time that both a general and a specific inhibitor of SKI-1 protease are able to coordinately block transcription of this group of mineralization related genes. Since inactivation or deletion of the *type XI collagen*, *type I collagen*, *Dmp1*, or *Phex* gene in vivo either causes a bone deficiency phenotype or abnormal skeletal development (2-5, 7, 8, 47, 48), we propose that their combined reduced transcription is the primary mechanism by which AEBSF and dec-RRLL-cmk inhibit mineralization in osteoblastic cultures.

An additional unexpected stimulatory effect of dec-RRLL-cmk on transcription of COL1A2 suggests that type I collagen may not be required for initial mineral crystal nucleation and deposition within BMF in the UMR106-01 model. Rather, the blockage of procollagen C proteinase enhancer protein activation by AEBSF (16), which facilitates procollagen processing and fibril assembly, leads us to propose that type I collagen may function during subsequent propagation and growth of initial mineral crystals in this model. However, additional studies are needed to confirm that these transcriptional changes reflect differences in protein content.

Consideration of the effects of AEBSF and dec-RRLL-cmk on gene expression in osteoblastic cells immediately raises questions about whether the promoters for *fibronectin*, *DMP1*, *Phex*, *COL11A1*, and *COL1A2* are regulated by SKI-1 activated transcription factors. A review of the literature indicates that only the *fibronectin* and positive control *HMG-CoA-Synthase* promoters are known to be regulated by CREB and SREBP-2 (42, 43, 49, 50). However, ECR Browser searches of the proximal 5-6 kb promoters for the human, mouse, and rat *fibronectin*, *Dmp1*, *Phex*, *COL11A1*, *HMG-CoA-Synthase*, and *COL1A2* genes revealed conserved CRE and SRE consensus sequences in all six promoters (data not shown). While these assignments do not ensure functionality, they are consistent with a common role for SKI-1 in regulating transcription of *fibronectin*, *Dmp1*, *Phex*, *COL11A1*, *COL1A2*, and *HMG-CoA-Synthase*.

Analysis of nuclear transcription factor content and size supports a role for SKI-1 in mineralization. The nuclear content of 58 kDa OASIS (CREB3L1) was decreased by AEBSF and dec-RRLL-cmk. These results are consistent with the known role of SKI-1 in activating OASIS. Furthermore, changes in the nuclear OASIS content brought about by AEBSF and dec-RRLL-cmk correlates well with changes both in the mineral content and with the expression of COL11A1, FN, Phex, and Dmp-1 in osteoblastic cultures.

AEBSF and dec-RRLL-cmk each affected the nuclear contents of 68 kDa activated SREBP-1 and SREBP-2 differently. However, as expected, caspase-3 cleaved forms of SREBP-1 (58 kDa) and SREBP-2 (65 kDa) were enriched in +FBS cultures. We presume that the cause for this change is serum cholesterol inhibition mediated by SCAP transport protein (41).

The response of SREBP-1 and SREBP-2 to Z-DEVD-fmk was also different. While the rationale for this finding is not clear, we suggest that SREBP-1 could be activated by another caspase not susceptible to this inhibitor or that turnover of SREBP-1 and SREBP-2 may follow distinct pathways.

In summary, the nuclear contents of activated OASIS, SREBP-1, and SREBP-2 were all reduced in AEBSF and dec-RRLL-cmk treated cultures relative to mineralizing controls. Since the proximal promoters for fibronectin, COL11A1, Phex, and Dmp-1 all contain SRE consensus sequences (data not shown), our results suggest that these inhibitors mediate their effects in osteoblastic cells by blocking activation and nuclear import of these SKI-1 activated transcription factors leading to their diminished nuclear contents and reduced transcription of *fibronectin*, *COL11A1*, *Phex*, and *Dmp-1*.

Although fibronectin, COL11A1, Phex, and Dmp-1 responded uniformly to the presence of SKI-1 inhibitors, COL1A2 expression reacted oppositely and increased over controls in response to dec-RRLL-cmk. We speculate that regulation of COL1A2 expression may be more complex and that our results may reflect the actions of non-SKI-

1 regulated transcription factors. However, it is interesting to note that despite an increase in COL1A2 expression, the overall effect of dec-RRLL-cmk was to block mineralization in UMR106-01 cultures.

Effects of inhibitors on caspase-3 activation and caspase-3 turnover. SREBP-1, SREBP-2, and CREB transcription factors all appear to be subject to proteasomal degradation (53, 54). Hirano et al. (53) showed that SREBP-1 is ubiquitinated and degraded in a manner consistent with the proteasome and that its 3 h half-life was increased when cells were treated with proteasome inhibitors. Interestingly, when ubiquitination was blocked, a small increase in nuclear SREBP-1 and SREBP-2 content was observed along with an increase in expression of HMG-CoA Synthase. Three sites on SREBP-1 are important in terms of its phosphorylation (Thr426 and Ser430 and Ser434). Interestingly, phosphorylation occurs after SREBP-1 binds to chromatin and is mediated by glycogen synthase kinase3-beta (55, 56) (see model, Fig. 9). Ubiquitin ligase Fbw7 is then recruited to SREBP-1/promoter complexes following its phosphorylation and catalyzes ubiquitinylation of lysines with subsequent proteasomal degradation of the modified SREBP-1. Based on this requirement and recent identification of its nuclear localization sequence (57), we have proposed that GSK3-β can be imported into the nucleus (see model, Fig. 9).

Because cytosolic caspase-3 can cleave adenomatous polyposis coli protein and β-catenin (58, 59), we speculate that a decrease in the intracellular content of activated caspase-3 could lead to an increase in cytosolic complexes of GSK3-β with APC and β-catenin (see model, Fig. 9). In this way, less GSK3-β would then be imported into the nucleus where it would phosphorylate SREBP-1 (and possibly SREBP-2 and OASIS)—leading to their ultimate proteasomal degradation. Thus, when caspase-3 is inactivated by Z-DEVD-fmk or when activation of caspase-3 is inhibited by dec-RRLL-cmk, more GSK3-β is predicted to remain complexed with axin, catenin, and APC protein in the cytoplasm (60), unable to phosphorylate transcription factors, thus decreasing their turnover and transiently increasing their nuclear concentration. In a similar way, caspase inhibitors Z-VAD-fmk and Z-DEVD-fmk were shown to block apoptosis by suppressing NF-kappa B/p65 degradation, thereby increasing nuclear translocation, DNA binding and transcriptional activity (61).

Direct Western blotting analyses demonstrated here that the level of activated 19 kDa caspase-3 subunit was reduced in dec-RRLL-cmk treated cultures. These findings are consistent the report by Park et al. (62) who showed that a serine protease was required to activate caspase-3 during apoptosis initiated by TNF-α. These results suggest that SKI-1, a serine protease, can mediate directly or indirectly the activation of procaspase-3 (see model, Fig. 9).

Although many studies have linked activation of SREBP-1 and SREBP-2 with ER stress and apoptosis (24), recent work has shown that SREBP activation is also a characteristic of differentiated cellular pathways such as membrane biogenesis associated with phagocytosis (63), the secretion of insulin by pancreatic beta cells (64), and the transcription of the low density lipoprotein receptor by endothelial cells induced by shear stress (65). Also SREBP-1c (ADD-1) (66) is a major positive regulator of fatty acid synthesis in developing adipogenic tissues. Our results showing that SKI-1 inhibitors block mineralization and the coordinated transcription of key mineralization related genes support a requirement for SKI-1 in the differentiation of osteoblastic cells. Prior evidence for a non-apoptotic role for caspase-3 in osteoblast differentiation was also presented by Mogi and Togari (67) and Miura et al. (68).

Our novel results demonstrate that a group of genes required for normal bone formation share a common transcriptional regulatory mechanism in mineralizing osteoblastic cells (see model, Fig. 9). Comparative Western blot analyses of the sizes and contents of transcription factors SREBP-1, SREBP-2, OASIS, and CREB-H in AEBSF or dec-RRLL-cmk treated cultures further support the role of SKI-1 in the activation of these transcription factors, and, implicitly, in the regulation of *COL11A1*, *Phex*, *Dmp1*, and *fibronectin*. Careful analyses of the effects of these inhibitors also indicate a hierarchical relationship in which SKI-1 or another serine protease inhibited by dec-RRLL-cmk, but not by AEBSF, catalyzes the activation of caspase-3 in osteoblastic cells. Our results indicate that the differentiated phenotype of osteoblastic cells, and possibly osteocytes, depends upon the non-apoptotic actions of SKI-1 to regulate the synthesis of proteins (and lipids for vesicles)

needed to assemble and mineralize the extracellular matrix of bone.

REFERENCES

1. Lian JB, Stein GS. 1992. Crit Rev Oral Biol Med. 3:269-305.
2. Ruchon AF, Tenenhouse HS, Marcinkiewicz M, Siegfried G, Aubin JE, DesGroseillers L, Crine P, Boileau G. 2000. J Bone Miner Res 15:1440-1450.
3. The HYP Consortium. 1995. Nature Genet. 11:130-136.
4. Lorenz-Depiereux, B, Bastepe, M, Benet-Pages, A, Amyere, M, Wagenstaller, J, Muller-Barth, U, Badenhoop, K, Kaiser, SM, Rittmaster, RS, Shlossberg, AH, Olivares, JL, Loris, C, Ramos, FJ, Glorieux, F, Vikkula, M, Juppner, H, Strom, TM. 2006. Nature Genet. 38: 1248-1250.
5. Feng, JQ, Ward, LM, Liu, S, Lu, Y, Xie, Y, Yuan, B, Yu, X, Rauch, F, Davis, SI, Zhang, S, Rios, H, Drezner, MK, Quarles, LD, Bonewald, LF, White, KE. 2006. Nature Genet. 38: 1310-1315.
6. Hansen U, Bruckner P. 2003. J Biol Chem. 278:37352-37359.
7. Li Y, Lacerda DA, Warman ML, Beier DR, Yoshioka H, Ninomiya Y, Oxford JT, Morris NP, Andrikopoulos, K, Ramirez F, et al. 1995. Cell 80:423-430.
8. Richards, AJ, Yates, JRW, Williams, R, Payne, SJ, Pope, FM, Scott, JD, Snead, MP. 1996. Hum. Molec. Genet. 5: 1339-1343.
9. Schneider GB, Zaharias R, Stanford C. 2001. J Dent Res. 80:1540-1544.
10. Moursi AM, Damsky CH, Lull J, Zimmerman D, Doty SB, Aota S, Globus RK. 1996. J Cell Sci. 109:1369-1380.
11. Moursi AM, Globus RK, Damsky CH. 1997. J Cell Sci. 110:2187-2196.
12. Stanford CM, Jacobson PA, Eanes ED, Lembke LA, Midura RJ. 1995. J. Biol Chem. 270:9420-9428.
13. Wang, A, Martin, JA, Lembke, LA, and Midura, RJ. 2000. J. Biol. Chem. 275:11082-11091.
14. Gorski JP, Wang A, Lovitch D, Law D, Powell K, Midura RJ. 2004. J Biol Chem. 279:25455.
15. Midura RJ, Wang A, Lovitch D, Law D, Powell K, Gorski JP. 2004. J Biol Chem. 279:25464.
16. Huffman NT, Keightley JA, Chaoying C, Midura RJ, Lovitch D, Veno PA, Dallas SL, and Gorski JP. 2007. J Biol Chem. 282:26002-26013.
17. Wang C, Wang Y, Huffman NT, Cui C, Yao X, Midura S, Midura RJ, Gorski JP. 2009. J Biol Chem 284:7100-713.
18. Gorski JP, Huffman NT, Cui C, Henderson E, Midura RJ, Seidah NG. 2009. Tissues, Cells, and Organs 189:25-32.
19. Seidah NG, Mayer G, Zaid A, Rousselet E, Nassoury N, Poirier S, Essalmani R, Prat A 2008. Int J Biochem Cell Biol. 40:1111-1125.
20. Wang X, Pai JT, Wiedenfeld EA, Medina JC, Slaughter CA, Goldstein JL, Brown MS. 1995. J Biol Chem. 270:18044-18050.
21. Wang X, Zelenski NG, Yang J, Sakai J, Brown MS, Goldstein JL. 1996. EMBO J. 15:1012-1020.
22. Higgins ME, Ioannou YA. 2001. J Lipid Res. 42:1939-1946.
23. Guan G, Dai PH, Osborne TF, Kim JB, Shechter I. 1997. J Biol Chem. 272:10295-102302.
24. Schröder M. 2008. Cell Mol Life Sci. 65:862-894.
25. Murakami T, Kondo S, Ogata M, Kanemoto S, Saito A, Wanaka A, Imaizumi K. 2006. J Neurochem. 96:1090-100.
26. Murakami T, Saito A, Hino S, Kondo S, Kanemoto S, Chihara K, Sekiya H, Tsumagari K, Ochiai K, Yoshinaga K, Saitoh M, Nishimura R, Yoneda T, Kou I, Furuichi T, Ikegawa S, Ikawa M, Okabe M, Wanaka A, Imaizumi K. 2009. Nature Cell Biol. 11:1205-1211.

27. Chandhoke TK, Huang YF, Liu F, Gronowicz GA, Adams DJ, Harrison JR, Kream BE. 2008. Bone
43:101-109.
28. Schlombs K, Wagner T, Scheel J. 2003. Proc Natl Acad Sci U S A. 100:14024-14029.
29. Patra D, Xing X, Davies S, Bryan J, Franz C, Hunziker EB, Sandell LJ. 2007. J Cell Biol. 179:687-
700.
30. Laemmli UK. 1970. Nature. 227:680-685.
31. Pullikotil P, Vincent M, Nichol ST, Seidah NG. 2004. J. Biol Chem. 279:17338-17347.
32. Pullikotil P, Benjannet S, Mayne J, Seidah NG. 2007. Biol Chem. 282:27402-27413.
33. Zhang K, Shen X, Wu J, Sakaki K, Saunders T, Rutkowski DT, Back SH, Kaufman RJ. 2006. Cell. 124:587-599.
34. Kalajzic I, Braut A, Guo D, Jiang X, Kronenberg MS, Mina M, Harris MA, Harris SE, Rowe DW.
2004. Bone. 35:74-82.
35. Kalajzic I, Kalajzic Z, Kaliterna M, Gronowicz G, Clark SH, Lichtler AC, Rowe D. 2002. J Bone Miner Res. 17:15-25.
36. Kalajzic I, Staal A, Yang WP, Wu Y, Johnson SE, Feyen JH, Krueger W, Maye P, Yu F, Zhao Y, Kuo L, Gupta RR, Achenie LE, Wang HW, Shin DG, Rowe DW. 2005. J Biol Chem. 280:24618-24626.
37. Pasquato A, Pullikotil P, Asselin MC, Vacatello M, Paolillo L, Ghezzo F, Basso F, Di Bello C, Dettin M, Seidah NG. 2006. J Biol Chem. 281:23471-23481.
38. Seidah NG, Mowla SJ, Hamelin J, Mamarbachi AM, Benjannet S, Touré BB, Basak A, Munzer JS, Marcinkiewicz J, Zhong M, Barale JC, Lazure C, Murphy RA, Chrétien M, Marcinkiewicz M. 1999. Proc Natl Acad Sci U S A. 96:1321-1326.
39. Elagoz, A, Benjannet, S, Mammarbassi, A, Wickham, L, and Seidah, NG. (2002) J. Biol. Chem. 277, 11265–11275.
40. Henrich S, Cameron A, Bourenkov GP, Kiefersauer R, Huber R, Lindberg I, Bode W, Than ME. 2003. Nat Struct Biol. 10:520-526.
41. Nohturfft A, Yabe D, Goldstein JL, Brown MS, Espenshade PJ. 2000. Cell 102:315-332.
42. Dooley KA, Bennett MK, Osborne TF. (1999) J. Biol Chem. 274:5285-5291.
43. Inoue J, Sato R, Maeda M. (1998). J Biochem. 123:1191-1198.
44. Chandler JM, Cohen GM, MacFarlane M. 1998. J Biol Chem. 273:10815-10818.
45. Liu X, Kim CN, Pohl J, Wang X. 1996. J Biol Chem. 271:13371-13376.
46. Omori Y, Imai J, Suzuki Y, Watanabe S, Tanigami A, Sugano S. 2002. Biochem Biophys Res Commun. 293:470-477.
47. Dixon PH, Christie PT, Wooding C, Trump D, Grieff M, Holm I, Gertner JM, Schmidtke J, Shah B,
Shaw N, Smith C, Tau C, Schlessinger D, Whyte MP, Thakker RV. 1998. J Clin Endocrinol Metab.
83:3615-3623.
48. Pihlajaniemi T, Dickson LA, Pope FM, Korhonen VR, Nicholls A, Prockop DJ, Myers JC. 1984. J
Biol Chem. 259:12941-12944.
49. Singh LP, Andy J, Anyamale V, Greene K, Alexander M, Crook ED. 2001. Diabetes. 50:2355-2362.
50. Michaelson JE, Ritzenthaler JD, Roman J. 2002. Am J Physiol Lung Cell Mol Physiol. 282:L291-301.
51. Starman, BJ, Eyre, D, Charbonneau, H, Harrylock, M, Weis, MA, Weiss, L, Graham, JM, Jr, Byers, PH. 1989. J. Clin. Invest. 84: 1206-1214.
52. Pastorino JG, Shulga N. 2008. J. Biol Chem. 283:25638-25649.
53. Hirano Y, Yoshida M, Shimizu M, Sato R. 2001. J Biol Chem. 276:36431-36437.

54. Costes S, Vandewalle B, Tourrel-Cuzin C, Broca C, Linck N, Bertrand G, Kerr-Conte J, Portha B, Pattou F, Bockaert J, Dalle S. 2009. Diabetes. 58:1105-1115.
55. Punga T, Bengoechea-Alonso MT, Ericsson J. 2006. J. Biol. Chem. 281:25278-25286.
56. Bengoechea-Alonso MT, Ericsson J. 2009. J Biol Chem. 284:5885-5895.
57. Meares GP, Jope RS. 2007. J. Biol Chem. 282:16989-167001.
58. Webb SJ, Nicholson D, Bubb VJ, Wyllie AH. 1999. FASEB J. 13:339-346.
59. Hunter I, McGregor D, Robins SP. 2001. J. Bone Miner Res 16:466-477.
60. Farr, G. H., 3rd, Ferkey, D. M., Yost, C., Pierce, S. B., Weaver, C. and Kimelman, D. (2000). J. Cell Biol. 148, 691-702.
61. Gupta S, Hastak K, Afaq F, Ahmad N, Mukhtar H. 2004. Oncogene 23:2507-2522.
62. Park IC, Park MJ, Choe TB, Jang JJ, Hong SI, Lee SH. 2000. Int J Oncol. 16:1243-1248.
63. Castoreno AB, Wang Y, Stockinger W, Jarzylo LA, Du H, Pagnon JC, Shieh EC, Nohturfft A. 2005. Proc Natl Acad Sci U S A. 102:13129-13134.
64. Amemiya-Kudo M, Oka J, Ide T, Matsuzaka T, Sone H, Yoshikawa T, Yahagi N, Ishibashi S, Osuga J, Yamada N, Murase T, Shimano H. 2005. Biol Chem. 280:34577-34589.
65. Liu Y, Chen BP, Lu M, Zhu Y, Stemerman MB, Chien S, Shyy JY. 2002. Arterioscler Thromb Vasc Biol. 22:76-81.
66. Gondret F, Ferré P, Dugail I. 2001. J Lipid Res. 42:106-113.
67. Mogi M, Togari A. 2003. J. Biol Chem. 278:47477-47482.
68. Miura M, Chen XD, Allen MR, Bi Y, Gronthos S, Seo BM, Lakhani S, Flavell RA, Feng XH, Robey PG, Young M, Shi S. 2004. J Clin Invest. 114:1704-1713.

ACKNOWLEGEMENTS

The authors wish to acknowledge the valuable technical assistance provided by Ms. Ellen Henderson and Pat Veno; Mr. Adnan Cheema provided important graphical support. JPG wishes to also thank the Bone Biology Group at UMKC for their long term support on this project and Dr. Tim Osborne, U. C. Irvine, for his generous assistance in analysis of SKI-1 activated transcription factors. JPG also wishes to thank Dr. Kezhong Zhang, Wayne State University, for providing anti-CREB-H antiserum. Supported by grant funds to JPG (NIH NIAMS R01-052775, UMKC Center of Excellence for Mineralized Tissues, and the University of Missouri Research Board); NGS was supported by a Canadian CIHR TEAM grant number CTP 82946. Funding from NIH NCRR P20RR016454 supported research infrastructure at Boise State University.

[6]ABBREVIATIONS

MGP, matrix GLA protein; SKI-1, site-1 or subtilisin/kexin isoenzyme-1; BGP, β-glycerolphosphate; SRE, sterol response element; CRE, cyclic AMP response element; S2P, site-2; BSP, bone sialoprotein; BAG-75, bone acidic glycoprotein-75; SDS PAGE; sodium dodecyl sulfate polyacrylamide gel electrophoresis; SAPE, streptavidin-phycoerythrin; GSK3-β, glycogen synthase kinase-3-beta; PC, proprotein convertase; AEBSF, 4-(2-aminoethyl) benzenesulfonyl fluoride hydrochloride; SREBP, sterol regulatory element-binding transcription factor; SCAP, SREBF cleavage activating protein; BMF, biomineralization foci; FBS, fetal bovine serum; MTT, 3-(4,5-dimethylthiazol-2-yl)-2,5-diphenyltetrazolium bromide; Z-DEVD-OPH, Z- Asp-Glu-Val-Asp-[2,6-difluorophenoxy]-methyl ketone; Z-DEVD-fmk, Z-Asp-Glu-Val-Asp-fluoromethyl ketone; dec-RRLL-cmk, decanoyl-Arg-Arg-Leu-Leu-chloromethyl ketone; FGF23, fibroblast growth factor 23; and, ICER, inducible cyclic AMP early repressor.

FIGURE LEGENDS

Figure 1. Activated 105 kDa SKI-1 is localized to extracellular calcified biomineralization foci in osteoblastic cultures.

A, Comparative Western blotting of laser micro dissected biomineralization foci with total cell layer extracts from osteoblastic cultures with anti-C-terminal SKI-1 antibodies. UMR106-01 osteoblastic cells were grown on glass slides, allowed to mineralize as described (13) and resultant mineralized biomineralization foci were isolated by laser micro dissection after staining with Alizarin red S dye; and isolated BMF and total cell layer fractions were then extracted and subjected to Western blotting as described previously (16). Six micrograms of protein was applied to each lane. No immunoreactive bands were detected in extraction buffer alone controls (Buffer, Fig. 1A). Numbers of left margin refer to estimated molecular weights of immunoreactive bands. **KEY: BMF**, biomineralization foci isolated by laser micro dissection; **CL-Min**, total cell layer from mineralized culture; **CL-UnMin**, total cell layer from non-mineralized culture; **Buffer**, control for extraction buffer.

B, Comparative Western blotting of cell layer extracts and media fractions from mineralized, AEBSF-inhibited, and non-mineralized osteoblastic cultures. Media was removed and the residual cell layer fraction was then extracted sequentially with 0.05 M EDTA and with 8M urea/0.5% CHAPS as described by Huffman et al. (16). Equivalent amounts of each fraction (urea/CHAPS extract, EDTA extract, and media) were subjected to Western blotting with anti-C-terminal SKI-1 antibodies using chemiluminescent detection. Numbers of left margin refer to estimated molecular weights of immunoreactive bands. **KEY: BGP**, with 6.5 mM β-glycerolphosphate; and, **AEBSF,** with 100 μM 4-(2-aminoethyl) benzene sulfonyl fluoride hydrochloride.

Figure 2. SKI-1 specific inhibitor, dec-RRLL-cmk, like AEBSF, specifically inhibits mineralization in UMR106-01 osteoblastic cultures.

Error bars refer to standard deviations; probabilities were determined by a one-way ANOVA with a Student-Newman-Keuls multiple comparison test.

A, Titration of dec-RRLL-cmk demonstrates its capacity to completely block mineralization without affecting cell viability. Osteoblastic cells were grown as usual and treated for 24 h under mineralizing conditions (see METHODS) with different concentrations of inhibitor. Mineralization was assayed with a colorimetric calcium assay by reference to a standard curve; cell viability was determined using the MTT assay.

B, Side-by-side comparison reveals dec-RRLL-cmk and AEBSF both completely block mineralization in culture. KEY: +BGP, plus β-glycerolphosphate; **-BGP**, minus β-glycerolphosphate; **dec-RRLL-cmk**, 40 μg/ml inhibitor; and, **AEBSF**, 100 μM inhibitor.
C, Furin peptide inhibitor dec-RVKR-cmk is without effect on mineralization. **KEY: +BGP,** plus β-glycerolphosphate; **-BGP**, minus β-glycerolphosphate; **dec-RVKR-cmk**, range of concentrations from 8 to 75 micromolar; and, **DMSO**, high and low represent solvent controls.

Figure 3. SKI-1 inhibitor dec-RRLL-cmk also blocks mineralization of primary mouse calvarial osteoblastic cells.
Primary mouse calvarial cells from transgenic DMP1 GFP mice (34) were harvested by a conventional sequential collagenase digestion protocol and plated as noted in METHODS. The media was changed at three day intervals starting on day 3 after plating. Some cultures were treated with SKI-1 inhibitors. Scale bars=375 microns
A, Control calvarial cells produced mineralized nodules on day 12 after plating. Mineralized nodules were detected by fluorescence microscopy after staining the culture with 10 μg/ml Alizarin red S dye. Green fluorescent signal represents GFP protein expressed under control of the 10 kb Dmp1 promoter. Yellow represents areas of overlap of mineral (red) and GFP signals. Arrows demark mineralized areas which also express GFP protein.
B, Dec-RRLL-cmk blocks the mineralization of primary calvarial cells as well as expression of GFP protein. Cells were treated continuously from day 3 until day 12 with 8 μM dec-RRLL-cmk inhibitor and then the cultures were imaged by fluorescence microscopy as in **A**.
C, AEBSF inhibits the mineralization of primary calvarial cells as well as expression of GFP protein. Cells were treated continuously from day 3 until day 12 with 10 μM AEBSF inhibitor and then the cultures were imaged by fluorescence microscopy as in **A**.

Figure 4. Dec-RRLL-cmk and AEBSF block expression by UMR106-01 osteoblastic cells of key genes required for mineralization and for normal bone formation.
Total RNA was isolated from replicate cultures (n=6/condition) treated for 12 h with β-glycerolphosphate with or without inhibitors and converted into cDNA with reverse transcriptase (see METHODS). Quantitative PCR was carried out using primer sets for individual genes and the relative expression for each gene was plotted as a percentage of that expressed by mineralized control cultures. Error bars refer to standard deviations and probabilities were calculated using a one-way ANOVA test. **KEY: +BGP**, control cultures treated with mineralizing conditions (6.5 mM β-glycerolphosphate); **+AEBSF+BGP**, cultures treated for 12 h with 100 μM AEBSF under mineralizing conditions; **+Dec-RRLL-cmk+BGP**; cultures treated for 12 h with 40 μM dec-RRLL-cmk under mineralizing conditions.

A-F, Quantitative PCR results for Dmp1, COL11A1, fibronectin, Phex, COL1A2, and HMGCS1 genes.

Figure 5. Dec-RRLL-fmk partially blocks activation of caspase-3 although caspase-3 inhibitors do not inhibit osteoblast-mediated mineralization.
UMR106-01 cultures were treated with β-glycerolphosphate with or without inhibitors and then cell layer fractions were assayed for soluble caspase-3 activity, mineral calcium content, and caspase-3 protein content by Western blotting as described in EXPERIMENTAL PROCEDURES. The direct effects of inhibitors on recombinant caspase-3 was analyzed separately. Error bars represent standard deviations and probabilities were tested with a one-way ANOVA test using a Student-Newman-Keuls multiple comparison test.
KEY: **Mineralized**, cells treated with β-glycerolphosphate; **Un-mineralized**, no β-glycerolphosphate; **+AEBSF**, cells treated with 100 μM inhibitor and β-glycerolphosphate; **+Dec-RRLL-cmk**, cells treated with 40-50 μM inhibitor and β-glycerolphosphate; **+ 10 Z-DEVD-fmk**, cells treated with 10 μM inhibitor and β-glycerolphosphate; **+ 20 Z-DEVD-fmk**, cells treated with 20 μM inhibitor and β-glycerolphosphate; **+ 10 Z-DEVD-OPH,** cells treated with 10 μM inhibitor and β-glycerolphosphate; **+ 20 Z-DEVD-OPH,** cells treated with 20 μM inhibitor and β-glycerolphosphate. All results are representative of at least duplicate experiments.

A, Treatment of UMR106-01 osteoblastic cultures with Z-DVED-fmk does not block mineralization. The average amount of calcium deposited in biomineralization foci was then determined colorimetrically (n=6).

B, Z-DVED-fmk and Dec-RRLL-cmk lead to significant reductions in intracellular caspase-3 activity. Soluble intracellular caspase-3 activity was extrapolated from kinetic reaction plots; the averaged data is plotted as Arbitrary Fluorescence Units/h (n=6).

C, Dec-RRLL-cmk does not directly inactivate recombinant caspase-3. Activity was extrapolated from kinetic reaction plots and is plotted as the average nmoles AMC released/h/ng protein (n=6).

D, Western blot analysis for precursor and activated caspase-3 forms. The amount of procaspase-3 32 kDa and of intracellular activated 19 kDa caspase-3 subunit varies depending upon the protease inhibitor treatment. The total cell layer of treated UMR106-01 cultures was extracted with hot SDS/urea sample buffer and subjected to Western blotting with anti-caspase-3 antibodies. The pattern is representative of triplicate experiments. **Arrow** denotes decreased 19 kDa band in dec-RRLL-cmk treated cells; **arrowheads** demark increased 19 kDa band content in cells which were treated with caspase-3 Z-DEVD-fmk or Z-DEVD-OPH inhibitor.

E, Western blot for intracellular GAPDH control. The cell layers in triplicate wells were extracted with hot SDS/urea sample buffer and subjected to Western blotting with anti-GADPH antibodies.

Figure 6. AEBSF, dec-RRLL-cmk, and Z-DEVD-fmk inhibitors alter the nuclear content of SKI-1 activated transcription factor(s).

Cultures were treated for 12 h under mineralizing conditions with different protease inhibitors and the nuclear fraction was then isolated. All culture conditions were carried out in triplicate and Western blotting results for OASIS, CREB-H, SREBP-1, and SREBP-2 depicted are representative of these replicates. Cytoplasmic fractions were also isolated from these same cultures and Western blots for control protein GAPDH are shown in Figure 7. All lanes shown for each different transcription factor were imaged similarly and at the same time. **KEY**: **Mineralizing**, cells treated with mineralizing conditions (6.5 mM β-glycerolphosphate); **No Phosphate**, no β-glycerolphosphate added; **+AEBSF**, cells treated with 100 μM inhibitor; **+Dec-RRLL-cmk**, cells treated with 40 μM dec-RRLL-cmk; **10 Z-DEVD-fmk**, cells treated with 10 μM inhibitor; **20 Z-DEVD-fmk**, cells treated with 20 μM inhibitor.

OASIS panel, nuclear fractions subjected to Western blotting for OASIS.
CREB-H panel, nuclear fractions subjected to Western blotting for CREB-H.
SREBP-1 panel, nuclear fractions subjected to Western blotting for SREBP-1.
SREBP-2 panel, nuclear fractions subjected to Western blotting for SREBP-2.

Figure 7. Cytoplasmic contents of selected SKI-1 activated transcription factors.

Cultures were treated for 12 h under mineralizing conditions with different protease inhibitors and then the cytoplasmic fraction was isolated from each using a commercial kit. All culture conditions were carried out in triplicate and results shown are representative of these replicates and GAPDH Western blots were used to control for intra-culture variations. Nuclear fractions were also isolated from these same cultures. All lanes shown on each panel below was imaged similarly and at the same time.
KEY: **Mineralizing**, cells treated with 6.5 mM β-glycerolphosphate; **No Phosphate**, no β-glycerolphosphate added; **+AEBSF**, cells treated with 100 μM inhibitor; **+Dec-RRLL-cmk**, cells treated with 40 μM dec-RRLL-cmk; **10 Z-DEVD-fmk**, cells treated with 10 μM inhibitor; **20 Z-DEVD-fmk**, cells treated with 20 μM inhibitor.

OASIS panel, cytoplasmic fractions subjected to Western blotting for OASIS.
CREB-H panel, cytoplasmic fractions subjected to Western blotting for CREB-H.
SREBP-1 panel, cytoplasmic fractions subjected to Western blotting for SREBP-1.
SREBP-2 panel, cytoplasmic fractions subjected to Western blotting for SREBP-2.
GAPDH panel, cytoplasmic fractions subjected to Western blotting for GAPDH.

Fig. 8. Over-expression of activated forms of SREBP-1a and CREB-H in UMR106-01 cells increases the number and clustering of mineralized biomineralization foci, respectively.

Forty hours after plating, cells were transiently transfected with plasmid in the presence of Metafectamine Pro and grown under standard mineralizing conditions (see METHODS). At 88 h, cultures were fixed with 70% ethanol, stained with Alizarin red S dye, and photographed using a fluorescence microscope. Mineralized BMF appear as white dots or clusters (arrows) under these conditions. Over-expression with activated OASIS, SREBP-1c, and SREBP-2 was without effect and indistinguishable from non-plasmid control cultures. Calcium assays revealed that SREBP-1c transfected cells deposited 1.32-fold more hydroxyapatite than non-plasmid control cells ($p<0.05$). Scale bar=500 μm.

Figure 9. Proposed intracellular mechanism of AEBSF, Dec-RRLL-cmk, and Z-DEVD-fmk effects on gene expression by osteoblastic cells.

Steps depicted in bold type are those suggested from experimental data presented here. Other parts of the model are derived from a variety of literature sources referenced in the Discussion section.

TABLE 1
The effect of Inhibitors on Total Cellular SKI-1 Peptidase Activity

Culture Condition	Peptidase Activity +/- STD (Arbitrary fluorescence units/ h / culture well) x 1000	Percent of Control	Statistical Significance
Mineralizing Control (+BGP)	1616 +/- 58.3	100% +/- 3.6	
+100 μM AEBSF +BGP	1161 +/- 145.0	71.8% +/- 12.5	$p<0.05$
+50 μM Dec-RRLL-cmk +BGP	986 +/- 125.6	61.0% +/- 12.7	$p<0.05$
+20 μM DEVD-OPH +BGP	1727 +/- 67.9	106.8% +/- 3.9	
+75 μM Dec-RVKR-cmk +BGP	1807 +/- 119.0	111.8% +/- 6.6	

Replicate cultures (n=6) were stopped 8 h after the addition BGP and SKI-1 assays carried out on total cell lysates as described in EXPERIMENTAL PROCEDURES. Data analyzed using a 1-way ANOVA with a Student-Newman-Keuls multiple comparison test. Representative of duplicate experiments.

TABLE 2
AEBSF blocks transcription of a number of key mineralization related genes in whole array study with UMR106-01 cells

Fold Change	**Gene symbol**	**Description**
-1.58	Hsd17b11	hydroxysteroid (17-beta) dehydrogenase 11
-1.59	Senp7	SUMO1/sentrin specific protease 7
-1.64	Adamtsl1	AdamTS1 like protease
-1.66	Phex	Phosphate regulating gene with homologies to endopeptidases on the X chromosome
-1.67	Casp4	Caspase 4
-1.77	Enpp3	Alkaline phosphodiesterase
-1.85	Fbn2	Fibrillin 2
-1.90	Enpp2	Ectonucleotide pyrophosphatase/ phosphodiesterase 2
-1.90	Tnc	Tenascin C
-1.91	pColA1 (I)	Procollagen, type I, alpha 1 chain
-1.94	Mitf	Microphthalmia-associated transcription factor
-1.97	Atp1a2	ATPase, Na+K+ transporting, alpha 2
-1.97	Tnn	Tenascin N
-1.98	Fn	Fibronectin 1
-2.10	Scn1a	Sodium channel voltage-gated, type 1 alpha
-2.13	pColA1(XI)	Procollagen, type XI, alpha 1 chain
-2.18	pColA2(I)	Procollagen, type I, alpha 2 chain
-2.28	Acss2	Acyl CoA synthetase short chain family member 2
-2.37	Serpini1	Serine (cysteine) peptidase inhibitor
-2.50	DMP-1	Dentin matrix protein-1
-2.55	pColA2(I)	Procollagen, type I, alpha 2 chain
-2.99	Matn3	Matrilin 3

FIGURE 1

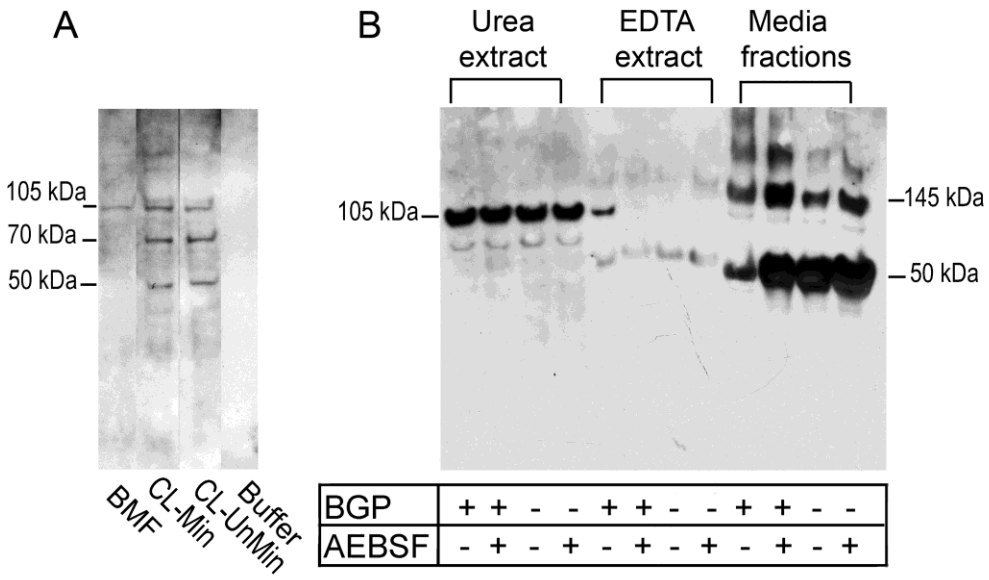

FIGURE 2

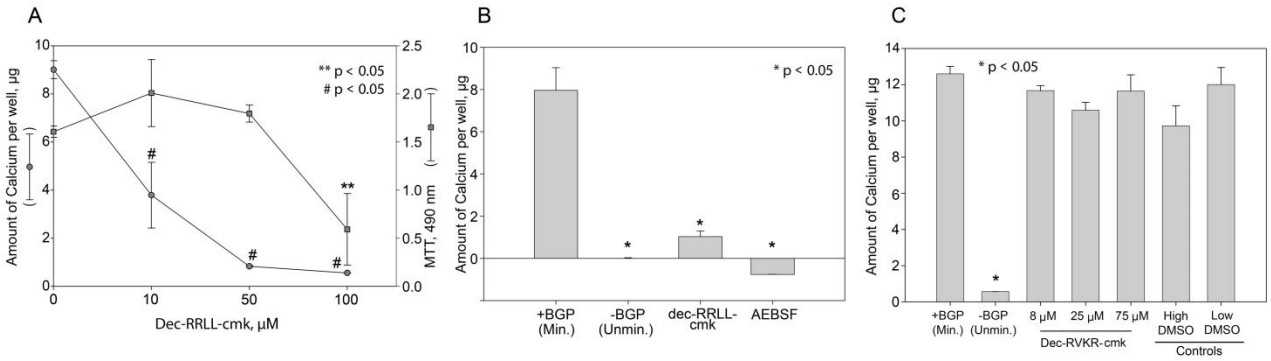

FIGURE 3

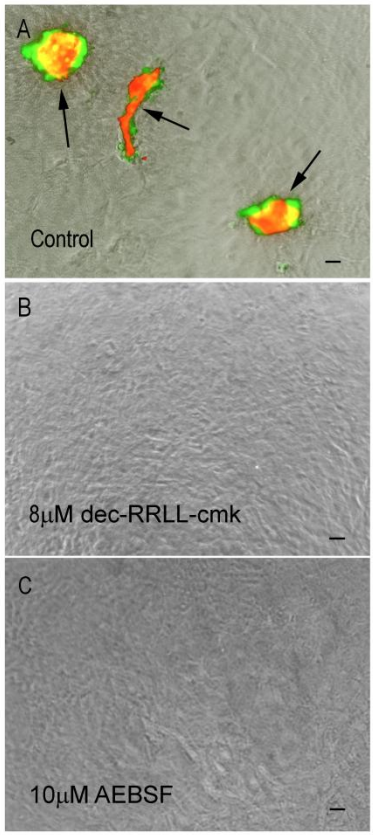

FIGURE 4

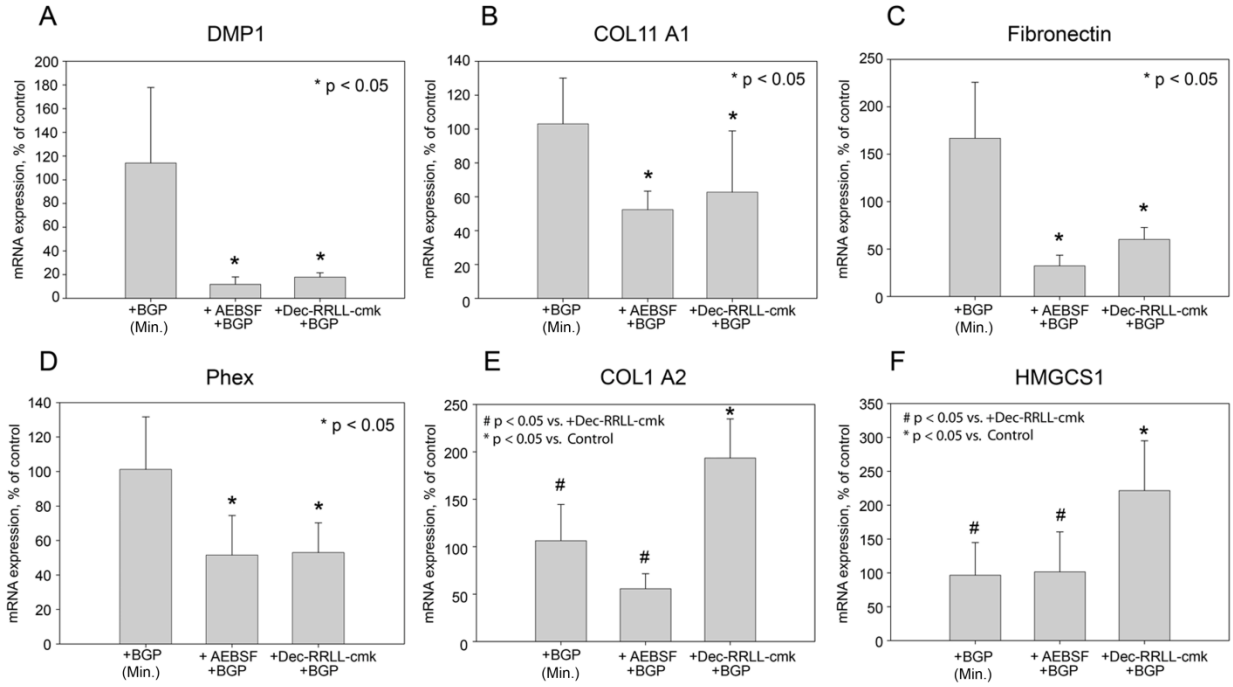

FIGURE 5

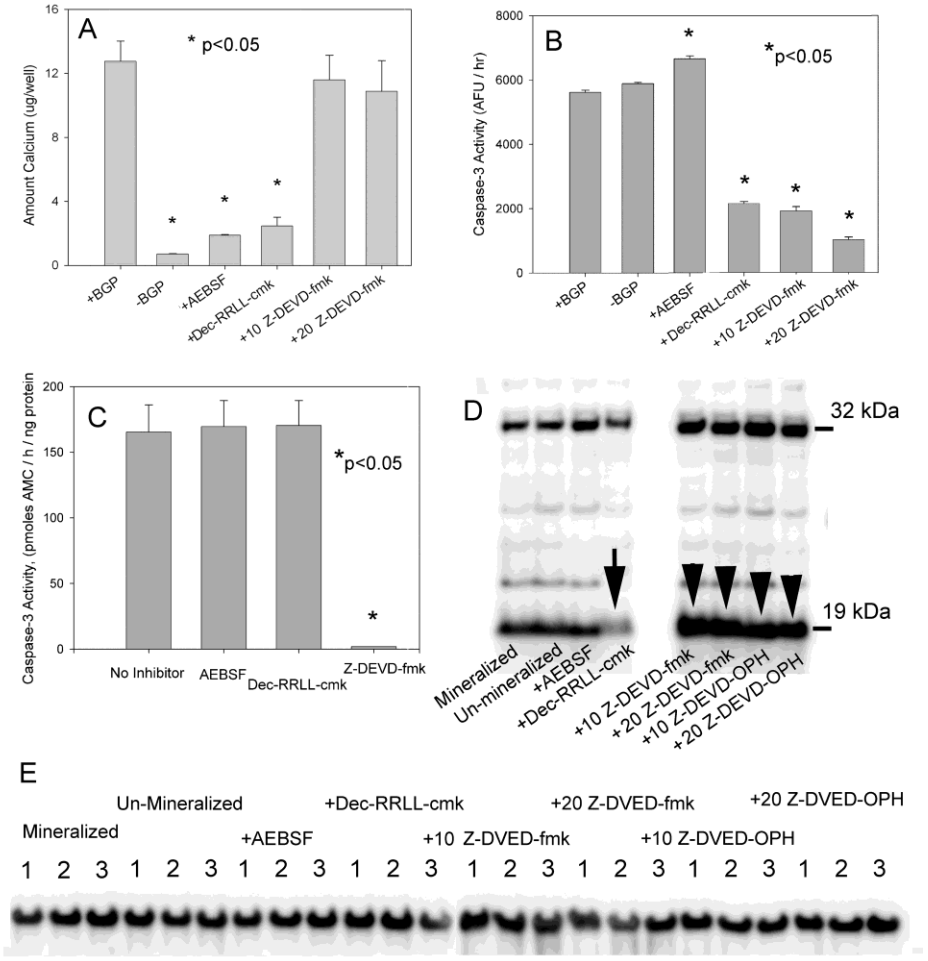

FIGURE 6

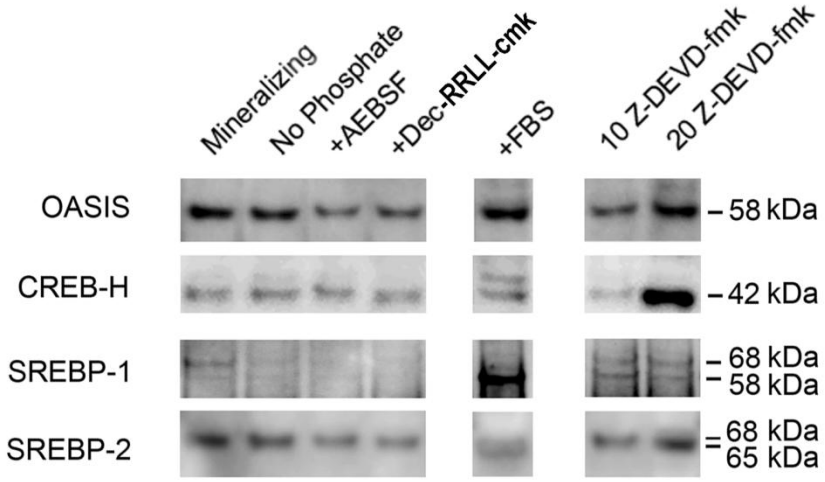

FIGURE 7

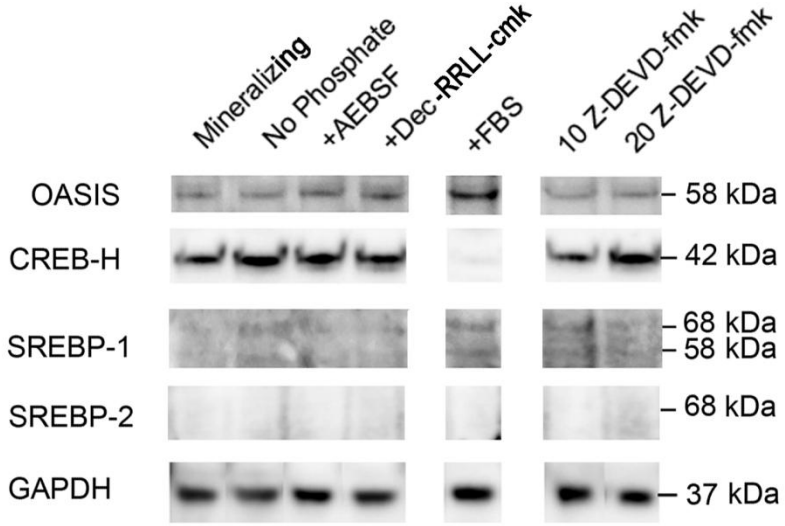

FIGURE 8

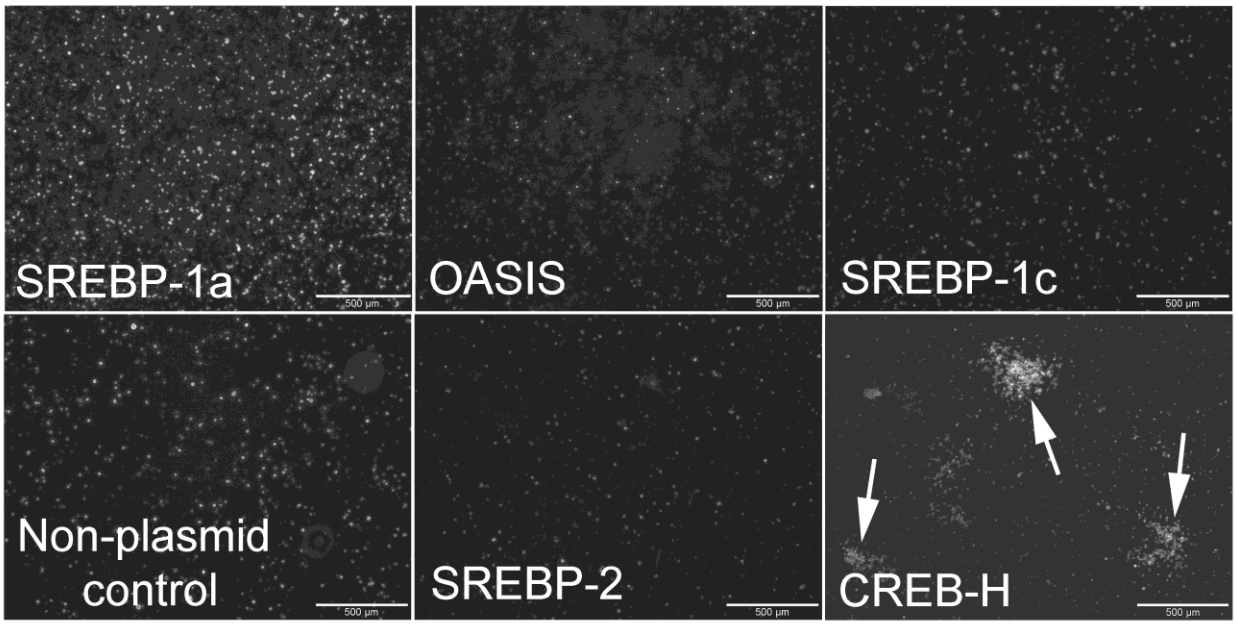

FIGURE 9